Title: Improvement of Arabidopsis biomass and cold-, drought-, and salinity-stress tolerance by modified circadian clock-associated PSEUDO-RESPONSE REGULATORs

Running Title: Regulation of biomass and stress responses by the clock

Corresponding Author: Norihito Nakamichi,

Institute of Transformative Bio-Molecules, Nagoya University, Furo-cho, Chikusa-ku, Nagoya 464-8601, Japan

Tel: +81-52-789-3656 (Ext. 3656)

Fax: +81-52-789-4778

Email: nnakamichi@itbm.nagoya-u.ac.jp

Subjective Areas: Environmental and stress responses

Number of black and white figures, color figures, tables and type and number of supplementary material:

Six color figures and three supplemental figures.

Title and running head: Improvement of Arabidopsis biomass and cold-, drought-, and salinity-stress tolerance by modified circadian clock-associated PSEUDO-RESPONSE REGULATORs

Authors: Norihito Nakamichi [1,2,3], Saori Takao [1], Toru Kudo [4, 5], Takatoshi Kiba [4], Yin Wang [1,6], Toshinori Kinoshita [1,2], and Hitoshi Sakakibara [4, 7]

Author's Address: [1] Institute of Transformative Bio-Molecules and [2] Graduate School of Sciences, Nagoya University, Furo-cho, Chikusa-ku, Nagoya 464-8601, Japan; [3] Precursory Research for Embryonic Science and Technology, Japan Science and Technology Agency, Kawaguchi, Saitama 332-0022, Japan; [4] RIKEN Center for Sustainable Resource Science, 1-7-22, Suehiro, Tsurumi, Yokohama 230-0045, Japan; [5] School of Agriculture, Meiji University, Kawasaki, 214-8571, Japan; [6] Institute for Advanced Research, Nagoya University, Furo-cho, Chikusa-ku, Nagoya 464-8601, Japan; [7] RIKEN Biomass Engineering Program Cooperation Division, 1-7-22, Suehiro, Tsurumi, Yokohama 230-0045, Japan.

Abbreviations: clock, Circadian Clock; CBF, C-repeat-binding factor; CDF, CYCLING DOF FACTOR; CO, CONSTANS; DREB1, dehydration-responsive element B1; eGO, enriched Gene Ontology; LD, long-day conditions; LL, constant light conditions; MS, Murashige and Skoog; PRR, PSEUDO-RESPONSE REGULATOR; TOC1, TIMING OF CAB EXPRESSION 1; ZT, Zeitgeber time.

Footnotes: Not be used in this study.

Abstract

Plant circadian clocks control the timing of a variety of genetic, metabolic, and physiological processes. Recent studies revealed a possible molecular mechanism for circadian clock regulation. *Arabidopsis thaliana* (Arabidopsis) *PSEUDO-RESPONSE REGULATOR* (*PRR*) genes, including *TIMING OF CAB EXPRESSION 1* (*TOC1*), encode clock-associated transcriptional repressors that act redundantly. Disruption of multiple *PRR* genes results in drastic phenotypes, including increased biomass and abiotic stress tolerance, whereas *PRR* single mutants show subtle phenotypic differences due to genetic redundancy. In this study, we demonstrate that constitutive expression of engineered PRR5 (PRR5-VP), which functions as a transcriptional activator, can increase biomass and abiotic stress tolerance, similar to *prr* multiple mutants. Concomitant analyses of relative growth rate, flowering time, and photosynthetic activity suggested that increased biomass of PRR5-VP plants is mostly due to late flowering, rather than to alterations in photosynthetic activity or growth rate. In addition, genome-wide gene expression profiling revealed that genes related to cold-stress and water-deprivation responses were upregulated in PRR5-VP plants. PRR5-VP plants were more resistant to cold-, drought-, and salinity stress than the wild-type, whereas *ft tsf* and *gi*, well-known late flowering and increased biomass mutants, were not. These findings suggest that attenuation of PRR function by a single transformation of PRR-VP is a valuable method for increasing biomass as well as abiotic stress tolerance in Arabidopsis. Because the *PRR* gene family is conserved in vascular plants, PRR-VP may regulate biomass and stress responses in many plants, but especially in long-day annual plants.

Key words; Circadian clock, biomass, PRR, *Arabidopsis thaliana*

Introduction

Recent changes in climatic and environmental conditions may require the use of biofuels from grass plant biomass as energy source for industrial purposes. It is therefore crucial to understand the molecular mechanisms associated with biomass production in grasses. Generally, it has been thought that improving photosynthetic capacity is the most efficient way to gain biomass. Indeed, increasing photosynthetic activity through modified regulation of stomatal opening results in increased biomass in *Arabidopsis thaliana* (Arabidopsis) (Wang et al., 2014), and increased stomatal conductance augments biomass production in wheat (Condon et al., 1987). Increasing photosynthetic activity by creating chloroplastic photorespiratory bypass also results in enhanced biomass in Arabidopsis (Kebeish et al., 2007).

Another possible way to improve biomass production is to increase net photosynthesis by augmenting total leaf area, which is controlled under tissue and organ developmental programs. Developmental processes that delay flowering time extend vegetative growth phase, allowing grasses to produce additional leaves and consequently greater biomass, including many annual plants species. Flowering time is often regulated by environmental cues, especially 'day-length' (Garner and Allard, 1920). Therefore, alternations of day-length delay flowering time, resulting in increased biomass production. Late flowering caused by genetic mutations also results in greater biomass (Redei, 1962; Kojima et al., 2002; Turner et al., 2005; Xue et al., 2008; Yuan et al., 2009; Yan et al., 2013). Collectively, late flowering and increased photosynthesis are the two ways known to increase biomass production.

In addition to enhancing photosynthesis, decreasing loss of photosynthesis capacity due to harmful environmental conditions is also important for biomass production. The most serious and frequent abiotic stress is drought (Mir et al., 2012), and about 45 million hectares of irrigated land contain excess salt. Under drought or high-salinity conditions, strong

tolerances against these stresses are required to maintain photosynthetic activity and biomass development among non-desert-adapted plants. It was also demonstrated that improving cold-, drought-, and salinity-stress responses by introducing Dehydration-responsive element B1/ C-repeat-binding factor (DREB1/CBF) and other key transcription factor genes enables plants to survive under water-stress conditions (Jaglo-Ottosen et al., 1998; Liu et al., 1998; Kasuga et al., 1999; Taji et al., 2002).

The circadian clock is a timekeeping system that coordinates biological processes with external day-night cycles to optimize fitness. The clock regulates various genetic, metabolic, and physiological rhythms (Chow and Kay, 2013), including photosynthetic activity, growth rate during vegetative growth phases (Dodd et al., 2005; Ni et al., 2009), flowering time, and abiotic- and biotic-stress responses, all of which are important processes for biomass production. Thus, the circadian clock could be a promising target for engineering biomass production. However, because current knowledge about how the clock regulates these physiological processes is limited, it is not easy to predict how we could optimize plant biomass by altering clock functions. In addition, it had been unclear whether two important physiological processes, namely flowering time regulation and the stress responses to cold, drought, and salinity, interact with each other.

Four Arabidopsis *PSEUDO-RESPONSE REGULATOR* (*PRR)* gene products (PRR9, PRR7, PRR5, and TOC1) have been proposed to regulate the circadian clock system by repressing clock-associated genes (Nakamichi et al., 2010; Nakamichi, 2011; Gendron et al., 2012; Huang et al., 2012; Wang et al., 2013), though another member of this gene family, PRR3, does not appear to be a part of this repression (Gendron et al., 2012; Nakamichi et al., 2012). PRR9, PRR7, and PRR5 directly repress genes in the clock output pathway, including the *CYCLING DOF FACTOR* (*CDF*) genes involved in flowering time control, and *DREB1/CBF* genes in cold stress responses (Nakamichi et al., 2012; Liu et al., 2013).

Multiple disruptions of *PRR9*, *PRR7*, and *PRR5* result in drastically altered phenotypes, such as late flowering, increased biomass production, and drought-stress resistance (Nakamichi et al., 2005; Nakamichi et al., 2007; Fukushima et al., 2009; Nakamichi et al., 2009), suggesting that *PRR* genes are promising targets for controlling biomass. However, single mutants of each *PRR* display subtle phenotypes, suggesting that these three Arabidopsis *PRR*s function redundantly. Genetic redundancy in *PRR* genes seems to be conserved among many plant species as evidenced by comprehensive phylogenetic studies (Takata et al., 2010), suggesting that generation of knock-out or down-regulation of multiple *PRR* genes, which takes time and effort, is necessary to test this idea in other plants. Therefore, development of a simple, one-step technology that could be used to inhibit *PRR* function could be of great utility.

We have established Arabidopsis transgenic lines expressing PRR5 fused to a construct of two tandem VP16 stringent transcriptional activation domains (PRR5-VP) under the control of a constitutive promoter (Nakamichi et al., 2012). PRR5-VP-expressing Arabidopsis plants display late flowering and long hypocotyl phenotypes, similar to those of *prr9 prr7 prr5* triple mutants, implying that PRR5-VP is a dominant negative regulator of endogenous PRR function. In this study, we demonstrate that transcriptional activators of PRR function as a dominant negative regulator of endogenous PRR function for biomass and responses to cold, drought, and salt-stress. PRR5-VP-expressing plants accumulated more biomass because of their extended vegetative growth phase, rather than by any increase in photosynthetic activity during the vegetative growth phase. In addition to effects on late flowering, we find that PRR5-VP plants show strong cold-, drought-, and salinity-stress tolerance, likely due to miss-expression of *DREB1* genes, which is not observed in late flowering mutants *ft tsf* and *gi*. Because *PRR* genes are conserved in many plants, our approach provides proof-of-concept in which the transcriptional activator types of PRR

proteins are valuable for delaying flowering time as well as abiotic stress tolerance, both of which contribute to biomass production, especially in long-day annual plants.

Results

Expression of PRR5-VP in Arabidopsis results in increased biomass

Because the circadian clock regulates photosynthesis (Dodd et al., 2005) and flowering time (Yanovsky and Kay, 2002), both of which are important for biomass production, we examined biomass production of clock-perturbed Arabidopsis plants, PRR5-VP-expressing Arabidopsis (PRR5-VP), the triple mutant *prr9 prr7 prr5*, and transgenic Arabidopsis lines expressing native *PRR5* (*PRR5-ox*). Aerial tissue dry-weight was measured after terminal flower production under long-day (LD, 16 h light/ 8 h dark) conditions. Biomass of PRR5-VP and *prr9 prr7 prr5* triple mutants was almost double that of wild-type, whereas that of *PRR5-ox* was about half that of wild type (Figure 1A).

To determine possible physiological processes for increased biomass in PRR5-VP, we concurrently examined leaf area, photosynthetic activity, and flowering time under LD. Wild-type and PRR5-VP plants started to bolt at about 25 and 34 days after germination (DAG), respectively, showing the late-flowering phenotype of PRR5-VP under LD (Figure 1B). Given that biomass is correlated with leaf area in Arabidopsis (Leister et al., 1999), we measured leaf area as biomass to examine biomass of growing plants. In wild-type, total leaf area per plant reached about 15 cm^2, when they started bolting on 25 DAG (Figure 1C and D). PRR5-VP grew slower than the wild-type within 25 DAG (about 5 cm^2), and continued to grow in the vegetative state, producing additional leaves with considerably more biomass (about 20 cm^2) by the time plants started to bolt (34 DAG) (Figure 1C and D). The growth rate of PRR5-VP from 25 DAG to 35 DAG was comparable to that of wild-type from 15 DAG to 25 DAG, and that of PRR5-VP before 25 DAG was lower than wild-type (Figure 1D).

Photosynthetic activity determined as CO_2 assimilation was examined in plants just before flowering (23 to 25 DAG for Wild-type, 32 to 34 DAG for PRR5-VP). The CO_2 assimilation rate of PRR5-VP was similar to the wild-type with photon flux densities of 100 $\mu mol \cdot m^{-2} \cdot s^{-1}$ (Student's t test $p > 0.05$) (Figure 1E). In addition, stomatal conductance of PRR5-VP was similar to wild-type at photon flux densities of 100 $\mu mol \cdot m^{-2} \cdot s^{-1}$ ($p > 0.05$) (Figure 1F). These results indicate that introduction of PRR5-VP causes growth retardation at early stages of vegetative growth, but it also increases biomass, likely due to the extended vegetative growth phase rather than to changing photosynthetic activity.

PRR5-VP and PRR7-VP extend vegetative growth

Differences in leaf surface area, photosynthetic activity, and flowering time of PRR5-VP indicated that delayed flowering is the major cause for an increased biomass phenotype. *PRR* genes in vascular plants fall into 3 clades (TOC1 clade, PRR5 and PRR9 clade, and PRR7 and PRR3 clade, though Arabidopsis PRR3 has weak DNA-binding activity (Gendron et al., 2012)). To test whether transcriptional activators of the TOC1 and PRR7 type (*i.e.* TOC1-VP and PRR7-VP) delay flowering time, we generated transgenic lines expressing TOC1-VP (TOC1-VP) and PRR7-VP (PRR7-VP) and assessed flowering times under LD (Figure 2A). TOC1-VP and PRR7-VP lines took longer to flower than wild type ($p < 0.01$). However, TOC1-VP and wild-type started bolting when plants had generated a similar number of leaves ($p > 0.1$), indicating that TOC1-VP and wild-type plants flower at a similar developmental stage. PRR7-VP started to flower after generating more leaves than wild type (Figure 2A), suggesting that PRR7-VP, but not TOC1-VP, is effective in extending vegetative growth in Arabidopsis under LD.

To examine how PRR5-VP and PRR7-VP extend flowering time, expression of clock regulated-genes related to flowering time were analyzed. As expected from their late

flowering phenotype, expression of the florigen *FT* in PRR5-VP and PRR7-VP was drastically down-regulated compared to wild-type under LD (Figure 2B). *FT* expression levels in TOC1-VP were intermediate between those of wild-type and PRR5-VP. The data indicate that PRR-VP plants alter flowering time through down-regulation of *FT* expression. Because PRR5-VP and PRR7-VP act as transcriptional activators in transient assays (Nakamichi et al., 2012), activate the target genes, and affect further downstream genes, we assumed that attenuation of *FT* is an indirect effect of PRR5-VP and PRR7-VP regulation.

Afternoon expression of *CO*, encoding a transcriptional activator of *FT* (Kobayashi et al., 1999) is crucial for *FT* expression (Imaizumi et al., 2003; Valverde et al., 2004). *CO* was expressed in the afternoon in wild-type (Figure 2C), but peak levels of *CO* were twice as high in TOC1-VP as in wild-type. The peak phase of *CO* expression in the afternoon was advanced in PRR5-VP, and the afternoon *CO* peak was diminished in PRR7-VP. Alternation of *CO* expression patterns might explain *FT* expression patterns and flowering time in PRR5-VP and PRR7-VP, but not in TOC1-VP. We next analyzed expression of *GI* and *FKF1*, which encode proteins activating *CO* and *FT* through degradation of CDF proteins repressing *CO* and *FT* transcription (Imaizumi et al., 2005; Sawa et al., 2007; Song et al., 2012). *GI* is also involved in the clock system (Hicks et al., 1996; Kim et al., 2007). *GI* was expressed in the afternoon in wild-type (Figure 2D). Peak levels of *GI* in TOC1-VP were similar to wild-type, but trough levels were higher. Expression of *GI* during daytime was lower in PRR5-VP compared to wild-type, and higher in the dark in PRR5-VP. *GI* expression was lower during daytime and higher during nighttime in PRR7-VP compared to wild-type. *FKF1* expression peak appeared in the afternoon in wild-type (Figure 2E). *FKF1* peak levels doubled in TOC1-VP, compared with wild-type. The *FKF1* peak phase was advanced in PRR5-VP. The *FKF1* peak occurred around dawn and its trough was in the morning in PRR7-VP. *GI* and *FKF1* expression in all

plants was correlated with *CO* expression, but expression of these genes in TOC1-VP could not explain *FT* expression in the plant.

CDF1, CDF2, CDF3, and CDF5 redundantly repress *CO* and *FT* expression (Fornara et al., 2009). These *CDF* family genes were expressed with peaks around dawn in wild-type (Figure 2F to I), and were up-regulated in TOC1-VP, PRR5-VP, and PRR7-VP. Up-regulation of *CDF2* and *CDF5* were similarly observed in all three transgenic lines. *CDF3* and *CDF1* were also up-regulated in the transgenic plants in the afternoon when *CDF* expression was low in the wild-type. *CDF3* and *CDF1* were up-regulated in PRR5-VP and PRR7-VP to a much higher level than in TOC1-VP.

These results indicate that TOC1-VP up-regulates *CDF* genes, alters *GI* and *FKF1*, slightly increases *CO*, but suppresses *FT*. The reduction of *FT* in TOC1-VP did not cause any delay of flowering time under LD. On the other hand, PRR5-VP and PRR7-VP delayed flowering time likely though up-regulation of *CDF* genes, alteration of *GI* and *FKF1*, and suppression of *CO,* which results in a reduction of *FT* expression. Collectively, PRR5-VP and PRR7-VP delay flowering time by partly activating *CDF* genes.

Transcriptome analysis of PRR5-VP Arabidopsis

The circadian clock regulates a wide-range of physiological processes. PRR proteins directly regulate the expression of genes encoding key transcription factors involved in flowering time, hypocotyl elongation, and cold-stress responses (Huang et al., 2012; Nakamichi et al., 2012; Liu et al., 2013). Therefore, PRR5-VP may further indirectly affect a number of clock output genes through the regulation of PRR target genes. To reveal genes affected by PRR5-VP, genes that were significantly up-regulated or down-regulated in PRR5-VP at ZT12 in 12 h light / 12 h dark cycles were surveyed in a previous transcriptional array (Nakamichi et al., 2012). Introduction of PRR5-VP resulted in 190 up-regulated genes

and 171 down-regulated genes. As analyzed by enriched Gene Ontology (eGO), 'response to cold' was the most enriched category of up-regulated genes, followed by 'transcription factor activity', 'nicotianamine biosynthesis', 'circadian rhythm', 'response to abscisic acid stimulus', 'response to water deprivation', and 'response to salt stress' (Figure 3A; $P < 10^{-5}$). 'Peroxidase activity', 'response to oxidative stress', 'endomembrane system', 'cell wall', and 'arsenate reductase activity' were significantly enriched among the down-regulated genes (Figure 3B; $P < 10^{-5}$).

PRR5-VP confers cold-, drought-, and salinity-stress tolerance

Microarray analysis showed that cold stress-, water deprivation-, and salt stress-responsive genes are highly represented among those affected by PRR5-VP. Expression of genes encoding proteins that protect plants from stress, such as chaperones, biosynthetic enzymes for osmolytes, and regulatory proteins implicated in signal transduction for stress responses, are occasionally induced by the stresses (Yamaguchi-Shinozaki and Shinozaki, 2006). To determine whether these gene expression differences attributable to PRR5-VP provided tolerance to cold stress, plants grown at 22˚C were subjected to a day of cold stress at -5˚C, then returned to 22˚C. PRR5-VP and *prr9 prr7 prr5* plants survived freezing while the wild-type did not (Figure 4A). *PRR5-ox* and wild-type were similarly sensitive to freezing. To evaluate tolerance to drought stress, 21 day-old plants were not watered for 16 days. Although only about 20% of wild type plants survived drought stress treatment, PRR5-VP, *prr9 prr7 prr5*, and *PRR5-ox* survived at a significantly higher rate (Figure 4B). Since plant size occasionally affects drought stress tolerance (Alpert, 2006), the smaller size of PRR5-VP may be responsible for part or all of the drought stress tolerance of PRR5-VP. To examine this possibility, the stress test was performed using similar-sized plants (Supplemental Figure 2A). PRR5-VP showed higher survival rate than wild type (Supplemental Figure 2B),

indicating that plant size is not the lone or most important determinant of drought stress tolerance in PRR5-VP. For tolerance to high salinity, plants were grown on Murashige and Skoog (MS) medium for 4 days after germination and transferred to MS containing 200 mM NaCl. Four days after transfer, bleaching rates were measured. Bleached plants were observed in the wild-type population, but less often in the PRR5-VP and *prr9 prr7 prr5* lines, indicating that these plants are more resistant to high salinity (Figure 4C). *PRR5-ox* was as sensitive as wild-type to salt stress. Together, these data show that the PRR5-VP plant line is more tolerant to cold stress, drought, and salt stress than wild type.

To understand the relationship between flowering time regulation and drought- and high salinity-stress responses, we performed stress tests for late flowering mutants, *ft tsf* and *gi*. *ft tsf* was slightly more tolerant to drought and high salinity stresses than wild-type, but more sensitive to these stresses than PRR5-VP or *prr9 prr7 prr5* (Figure 4D and E). *gi* was similar in its drought- and high salinity- stress tolerance rates to *ft tsf* (Figure 4D and E). These results indicate that late flowering does not enhance drought and salt stress responses, and that the strong drought- and high salinity tolerance of PRR5-VP is independent from flowering time regulation.

PRR5-VP activates a DREB1-dependent pathway

Many cold stress-responsive genes are activated by DREB1/CBF transcription factor, and overexpression of this gene results in increased tolerance to cold-, drought- and high salinity-stresses (Jaglo-Ottosen et al., 1998; Liu et al., 1998; Kasuga et al., 1999). Because *DREB1* genes are directly repressed by PRR5 (Nakamichi et al., 2012), we tested whether *DREB1* genes are activated by PRR5-VP using the expression of three *DREB1* genes under 12 h light / 12 h dark and constant light (LL) conditions (Figure 5A). Three *DREB1* genes reached maximal expression levels around ZT9 under 12 h light / 12 h dark conditions,

and subjective dusk under LL, as described previously (Harmer et al., 2000; Fowler et al., 2005). The expression of *DREB1* genes at each time point was higher in PRR5-VP plants than wild-type, indicating that PRR5-VP activates *DREB1* expression (Figure 5A). To examine whether up-regulation of *DREB1* further influences downstream genes, we surveyed expression of three *DREB1* genes and 37 DREB1A-downstream genes (Maruyama et al., 2004) in a microarray data set (Figure 5B). Among 37 DREB1A-downstream genes, 16 were significantly up-regulated in PRR5-VP plants compared to wild-type at least at one time point (FDR $q < 0.01$), suggesting that PRR5-VP influences expression of DREB1A-downstream genes through *DREB1A* (Figure 5B). Other genes downstream of *DREB1* may be up-regulated (Figure 5B). In late flowering mutants *ft tsf* and *gi*, *DREB1* gene expression at ZT 0.5 and ZT 6.5 was similar to wild-type (Figure 5C). Collectively, these data suggest that PRR5-VP is more tolerant to cold-, drought-, and salt-stress due to altered expression of the *DREB1* genes. This result also suggests that late flowering time does not cause mis-expression of *DREB1* genes.

Discussion

Delaying flowering time causes increased biomass

The demand for biomass-based energy sources is growing (Fargione et al., 2008). Delaying flowering time, which is a major determinant of grass plant biomass can be used to meet some of that demand. In this study, we show that delaying flowering time can be achieved with a single transformation of PRR5-VP in a long-day plant, Arabidopsis (Figure 1). We propose that one reason for delayed flowering time in PRR5-VP plants is attenuation of florigen gene (*FT*) expression, likely through changing expression of genes regulating *FT* (e.g, *CDF*s, *CO*) (Figure 2). Previous studies indicate that mutants of *PRR* orthologues flower late in long-day plants (Nakamichi et al., 2005; Turner et al., 2005; Pin et al., 2012), but because there seems

to be extensive genetic redundancy of *PRR* genes in many plants, attenuation of multiple *PRR* genes may be required for pronounced extension of vegetative growth. We succeeded in overcoming this redundancy by expressing PRR5-VP in Arabidopsis (Figure 1). Alternatively, this study may meet a proof-of-concept standard for utility of PRR5-VP for increasing biomass by delaying flowering time, especially in long-day annual plants. Although single mutations of *PRR* orthologues in barley and beet result in late flowering (Turner et al., 2005; Pin et al., 2012), attenuation of redundant *PRR* functions by introduction of PRR-VP may delay flowering time further in these long-day plants.

On the other hand, in short-day plants, homologues of *PRR* delay flowering time. *Hd2* and *SbPRR37* from the short day plants rice and sorghum have high sequence homology to *PRR7* and both delay flowering (Murphy et al., 2011; Koo et al., 2013; Yan et al., 2013). In addition, our preliminary tests suggest that introduction of PRR5-VP into rice did not result in increased biomass (data not shown). Therefore, just increasing PRR activity might delay flowering and increase biomass in short-day plants, though this idea needs to be tested under rigorously controlled conditions.

Differences between PRR5-VP, PRR7-VP and TOC1-VP for delaying flowering time

Our results suggest that there are slight differences in the influence of clock outputs (expression of genes involved in flowering time) between TOC1 and PRR5/7 (Figure 2). Though the exact molecular mechanism for the difference is not clear, one possible explanation is that there is a difference in target gene recognition between PRR5/7, and TOC1. Indeed, comparisons of ChIPseq data imply that PRR5 and PRR7 associate with the upstream region of *CDF1* more frequently than TOC1 does (Huang et al., 2012; Nakamichi et al., 2012; Liu et al., 2013) (Supplemental Figure 3). In addition, expression patterns of *GI*, *FKF1*, and *CO* were different in TOC1-VP than in PRR5-VP and PRR7-VP, indicating different

activities of TOC1-VP and PRR7/PRR5-VP in Arabidopsis (Figure 2). Because three clades of *PRR*s (*TOC1* clade, *PRR3/PRR7* clade, and *PRR5/PRR9* clade) diverged before the branching between dicots and monocots (Takata et al., 2010), the different activities of PRR-VP observed in Arabidosis may be applicable in other long-day plants.

Delaying flowering time does not cause strong cold-, drought-, and salinity-stress tolerance

We found that PRR5-VP is resistant to cold-, drought-, and salinity-stresses, likely due to aberrant expression of *DREB1* genes and activation of additional downstream genes involved in these stress responses (Figures 4, 5, and Supplemental Figure 2). Although *DREB1* genes are activated in PRR5-VP, expression of *ICE1*, encoding an activator of *DREB1* in response to cold stress (Chinnusamy et al., 2003), was not up-regulated in PRR5-VP (Supplemental Figure 4), indicating that PRR5-VP activates *DREB1* without regulation of *ICE1*. Thus *DREB1* genes act as the nexus for converging two independent signaling networks: cold-stress response and circadian clock, partly through ICE1 and PRR.

Our study also revealed that *ft tsf* and *gi* late flowering mutants are not as tolerant to drought and high salt concentrations as PRR5-VP or *prr9 prr7 prr5* (Figure 4). PRR5-VP induces *DREB1* and downstream genes, including those encoding proteins that protect cells from cold stress (Figure 5). The up-regulation of DREB1-downstream genes may explain the stress tolerance phenotypes of PRR5-VP. On the other hand, mutations in *ft tsf* or *gi* did not up-regulate *DREB1*, and plants carrying these mutations did not show strong drought- or high salinity-stress tolerance (Figures 4 and 5). However, a QTL study suggests that late flowering time is associated with tolerance to moderate drought stress in *Arabidosis* (Schmalenbach et al., 2014), and stomata of *ft tsf* and *gi* are not fully opened even under blue light conditions (Kinoshita et al., 2011; Ando et al., 2013; Kimura et al., 2015), thus these late flowering

mutants might be tolerate to moderate drought stress, partly by closing stomata. We found that *PRR5-ox* is more tolerant to drought stress, but not to cold- or high salinity-stresses. The mechanism of this unexpected *PRR5-ox*-related drought stress tolerance should be addressed in a future study.

Recently, it was also demonstrated that *DREB1* expression is up-regulated in *gi* (Fornara et al., 2015). We also found slight up-regulation of *DREB1B* in *gi* at ZT 0.5 in this study (Figure 5C), but this up-regulation is not as great as in PRR5-VP and *prr9 prr7 prr5* (Figure 5C). Because GI interacts with proteins whose functions are divergent (e.g., SPINDLY, dynamin, *ZEITLUPE*, protein kinase) (Tseng et al., 2004; Kim et al., 2007; Abe et al., 2008; Kim et al., 2013), any effect of GI on *DREB1* gene expression may be minor. In contrast, PRR5-VP can compete with native PRR proteins as repressors for *DREB1* genes. This direct action of PRR5-VP on *DREB1* may explain why PRR5-VP is more effective as an up-regulator of *DREB1* than *gi* mutations.

Over-expression of *LOV KELCH PROTEIN 2* (*LKP2*), a homologue of *ZEITLUPE* (*ZTL*) and *FKF1* confers drought stress tolerance due to activation of *DREB1* genes (Miyazaki et al., 2015). Given that LKP2 degrades PRR5 protein redundantly with ZTL and FKF1 (Baudry et al., 2010), this approach might also confer drought stress tolerance through degradation of PRR5 (Nakamichi et al., 2012).

Although PRR5-VP plants are more tolerant to drought stress, it is not clear whether or not this stress tolerance contributes to biomass production under non-stress laboratory conditions. However, drought tolerance may contribute to biomass production in the field, since hydration conditions under cultivation can be highly variable. Given that over-expression of *DREB1B* (*CBF1*) resulted in late flowering though the gibberellin signaling pathway (Achard et al., 2008), PRR5-VP possibly affects flowering time though the pathway, as well as the CO-FT pathway. This hypothesis will be future consideration.

Possible additional approaches to increase biomass

It is likely that a combination of delayed flowering and increased photosynthetic activity would be an efficient way to meet some of the demand to increase biomass per plant. Indeed, increased photosynthetic activity resulting from altering stomatal opening results in increased biomass (Wang et al., 2014). The circadian clock regulates photosynthetic activity and total biomass (Dodd et al., 2005), but the molecular mechanism or mechanisms underlying regulation of photosynthetic activity by the clock are only partially understood. In this study, we found that photosynthetic activity, stomatal conductance, and growth rates during early vegetative growth phase were not higher in PRR5-VP than in wild-type, but rather the growth rate of PRR5-VP was lower than wild-type during early vegetative growth phase (Figure 1). This lower growth rate may be not due to any differences in photosynthetic activity per unit area of photosynthetic organ, but to the slender shape of leaf blades, which is also observed in *prr9 prr7 prr5* mutants (Niinuma et al., 2008). The slender leaf shape of *prr* mutants is likely caused by mis-expression of *PHYTOCHROME INTERACTING FACTOR4* (*PIF4*) and *PIF5*, which enhance shade avoidance response (Kunihiro et al. 2011; Niinuma et al. 2008; Niwa et al. 2009; Takase et al. 2013). In addition, because overexpression of *DREB1A* results in severe growth retardation (Liu et al., 1998), up-regulation of *DREB1* genes may be why growth is inhibited in PRR5-VP plants. eGO analysis indicates that 'peroxidase activity' and 'response to oxidative stress' are enriched in down-regulated genes in PRR5-VP (Figure 3), so PRR5-VP plants may be sensitive to oxidative stress. Thus, the strategy of introducing PRR5-VP may have a trade-off between late flowering/drought stress response, and slender shape/oxidative stress response in Arabidopsis. To overcome potential unfavorable phenotypes resulting from introduction of PRR5-VP, understanding the

functional effects of direct or indirect downstream genes in PRRs is an important future consideration.

In addition to understanding the downstream target genes of PRRs, external regulation of PRR5-VP would be another way to avoid negative effects of PRR5-VP. For example, since young seedlings of PRR5-VP had lower growth rates (Figure 1D), induction of PRR5-VP from 10 to 15 days after germination under the control of a chemically induced promoter may obviate growth retardation in an earlier growth phase. Because clock-output pathways are distinctly regulated in different tissues (Endo et al., 2014), induction of PRR5-VP in specific tissues or appropriate cells using tissue-specific promoters would be another way to avoid unfavorable phenotypes due to PRR5-VP. Collectively, spatial and temporal optimization of PRR5-VP induction is an interesting method, which could be developed to improve plant biomass.

Conclusion

Given that the circadian clock regulates many physiological processes, it is not easy to optimize plant biomass production by modification of the clock, and especially by manipulating a single gene. In this study, however, we showed that introduction of PRR5-VP can delay flowering time as well as increasing cold-, drought-, and salinity-stress tolerance, likely through up-regulation of PRR-direct target genes (*CDF*s and *DREB1*s), and further regulation of their downstream genes (Figure 6), which contribute to increased biomass. Because *PRR* genes are conserved in vascular plants, and functions of *PRR* for flowering time are similar in long-day plants, our approaches have potential to control flowering time and eventually biomass in these plants.

Materials and Methods

Plant materials and growth conditions

Ecotype accession Columbia-0 (Col-0) was used as the wild-type *Arabidopsis thaliana*. *prr9 prr7 prr5* triple mutants (Nakamichi et al., 2005), *PRR5-ox* (Sato et al., 2002), PRR5-VP (Nakamichi et al., 2012), *ft tsf* and *gi* (Ando et al., 2013) were described previously. To generate the PRR7-VP construct, the full length *PRR7* coding region, including introns, without a termination codon was amplified from Arabidopsis genomic DNA with the primer set 5'-CACCATGAATGCTAATGAGGAGGG-3', and 5'-GCTATCCTCAATGTTTTTTATGTC-3', and cloned into pENTR/D-TOPO (Life Technologies), generating pENTR/D-PRR7. The pENTR/D-PRR7 was incubated with Gateway LR clonase enzyme (Life Technologies) and pBS-35S-VP vector (Nakamichi et al., 2012) to generate pBS-PRR7-VP. The *PRR7-VP* region was amplified using the primer set 5'-CACGGGGGACTCTAGAATGAATGCTAATGAGGAGGG-3', and 5'-TTCGAGCTGCGGCCGCCTACCCACCGTACTC-3', and cloned into binary vector pSK1 (Kojima et al., 1999) between *Xba*I and *Not*I sites using an In-Fusion HD kit (Takara, Japan), generating pSK1-PRR7-VP. pSK1-PRR7-VP was used to transform Col-0 *via* an *Agrobacterium*-mediated method (Bechtold et al., 1993). To generate the TOC1-VP construct, the coding region of *TOC1* without introns or termination codon was cloned into pENTR/D-TOPO using primers 5'-CACCATGGATTTGAACGGTGAGTG-3', and 5'-AGTTCCCAAAGCATCATCC-3', generating pENTR/D-TOC1. pENTR/D-TOC1 was used to generate pBS-TOC1-VP by LR clonase as described above. *TOC1-VP* was amplified with the primers 5'-CACGGGGGACTCTAGAATGGATTTGAACGGTGAGTG-3', and 5'-TTCGAGCTGCGGCCGCCTACCCACCGTACTC-3' and cloned into pSK1. pSK1-TOC1-VP was transformed into Col-0. Ten independent transgenic T1 plants were selected, and the VP fusion proteins in two independent T2 plants were confirmed by Western blotting (Supplemental Figure 1). Plants were grown on MS (Murashige and Skoog, 1962)

containing 2 % (wt/vol) sucrose and 0.3 % gellan gum with or without 20 $\mu g \cdot L^{-1}$ of Hygromycin B, under 12-h light/12-h dark conditions (70 $\mu mol \cdot s^{-1} \cdot m^{-2}$).

Western blotting

Tissue samples (200 mg) from PRR7-VP, TOC1-VP, and Col-0 Arabidopsis grown under 12 h light /12 h dark conditions were frozen in liquid nitrogen at ZT12. Western blots were performed using anti-VP16 antibody (ab4808; Abcam) as described previously (Nakamichi et al., 2010).

Measurement of flowering time and biomass

Flowering time measurements were done as described previously (Nakamichi et al., 2012). Arabidopsis plants were grown under LD conditions (16 h light / 8 h dark) in a growth room until plants generated terminal flowers, at which time the aerial parts were harvested and dried for 3 days at 80 ˚C, and tissue dry-weight was measured. Plant biomass was determined as the total dry-weight of harvested plants (Figure 1A). Aerial parts were measured by Image J (http://imagej.nih.gov/ij/) as described (Leister et al., 1999) (Figures 1C and D).

Measurement of Gas-Exchange

Gas-exchange measurements were performed with an LI-6400 system (Li-Cor) as described previously (Wang et al., 2014). Plants were grown under LD conditions until just before a flowering bud was generated, then transferred into a dark room overnight. Photosynthetic activity and stomatal conductance were measured at 24˚C (Wang et al., 2014). Light intensity was set to 100 $\mu mol \cdot m^{-2} \cdot s^{-1}$, CO_2 concentration was set to 400 $\mu L\ L^{-1}$, and relative humidity of the chamber for leaf samples was 40 to 50 % (Pa/Pa).

Gene expression analysis

Plants were grown on MS containing 2 % sucrose for 10 days after germination under LD (for Figure 2), or 14 days after germination under 12 h light / 12 h dark conditions (Figure 5). RNA from Arabidopsis was prepared using an RNeasy Plant Mini Kit (Qiagen). Real-time reverse transcription followed by quantitative PCR (RT-qPCR) was performed as described previously (Nakamichi et al., 2010) using an Applied Biosystems StepOnePlus Real-Time PCR system (Life Technologies). Primers for qPCR for *APX3* (Nakamichi et al., 2010), for *FT*, *CO*, *GI*, and *FKF1* (Nakamichi et al., 2007) for *CDF5* (Nakamichi et al., 2012), for *DREB1* genes (Nakamichi et al., 2009) were used. Primers for *CDF* genes were *CDF1* (5'-ATGCTGGAAACTAAAGATCCTGC -3', and 5'- CAGAACTTAGTCTCCATGCTG -3'), *CDF2* (5'- GATGATGATGAAGAGATGGGTG -3', and 5'-CAGTTATACCCGATGTAGTAGTAG -3'), and *CDF3* (5'-GATGGAGACTAGAGATCCAGC -3', and 5' GGTTTCGGGTTTCGAATTGTTAAAAC -3').

Stress tests

For cold stress tests, seeds were sown on a mixture of 60% soil (Kumiai Nippi engeibaido, Nihon Hiryo, Tokyo) and 40% vermiculite supplemented with a 1/5000 dilution of HYPONEX (HYPONEX-JAPAN, Osaka). Plants were grown for 22 d under LD conditions at 23˚C in the growth chamber (LPH-410SP, NK system), then transferred to -5 ˚C (LP-50P, NK system) for 1 d, then returned to 23˚C. Survival rates were determined four days later. For the drought stress test outlined in Figure 4B, plants were grown under LD at 23˚C for 21 d, and left unwatered for 16 d. Then plants were watered for 4 d, and living plants were counted . For the drought stress test in Figure 4D, plants were grown on soil for 25 d, and left unwatered for 17 d. For the drought stress test in Supplemental Figure 2, similar-sized plants

(15 d after germination, and 8 d after germination for PRR5-VP and wild-type, respectively) were not watered for 14 d or 16 d. After the drought period, plants were watered for 4 d, and survival rates were determined. High salinity stress tests were done as described previously (Nakamichi et al., 2009).

Microarray data analysis and eGO analysis

Up-regulated and down-regulated genes at ZT12 in PRR5-VP were compared to wild-type expression (FDR $q < 0.01$) as described previously (Nakamichi et al., 2012). Row data for microarrays were deposited in the Gene Expression Omnibus (GEO) database www.ncbi.nlm.nih.gov/geo (accession no. GSE36360). Heat maps were generated with bioconductor of R (www.r-project.org) as described previously (Fukushima et al., 2009). eGO analysis was performed as described previously (Tsukagoshi et al., 2010).

ChIPseq data analysis

ChIPseq Sequence Read Archive (SRA) files of PRR7-HA (GSM1196649 of GSE49282) (Liu et al., 2013), and TOC1-YFP (GSE35952) (Huang et al., 2012) were obtained from the Gene Expression Omnibus (GEO) database. SRA files were converted into FASTA files with NCBI SRA Toolkit 2.2.2 (http://trace.ncbi.nlm.nih.gov/Traces/sra/std). Sequence reads were mapped to a Arabidopsis reference genome (TAIR10) by Bowtie 0.12.7 (Langmead et al., 2009), generating Sequence Alignment/Map (SAM) files. The SAM file for PRR5-GFP ChIP experiment was obtained from a previous study (GSE36361) (Nakamichi et al., 2012). All SAM files were converted into Binary Alignment/Map (BAM) format files by Samtools 0.1.18 (Li et al., 2009). BAM files and Indexed BAM files were used for visualization of mapping patterns by Integrative Genomics Viewer (IGV) 1.5.64.

Funding

This work was supported by Japan Science and Technology Agency Precursory Research for Embryonic Science and Technology Grant (20109), Japan Society for the Promotion of Science (24770042), and RIKEN Technology Transfer Office Fund to N.N.

Disclosures

The authors have no conflicts of interest to declare.

Acknowledgements

We thank S. Aoki, S. Suzuki, J. Inaba, and H. Ojima (RIKEN) for technical support.

References

Abe, M., Fujiwara, M., Kurotani, K., Yokoi, S., and Shimamoto, K. (2008). Identification of dynamin as an interactor of rice GIGANTEA by tandem affinity purification (TAP). Plant Cell Physiol **49,** 420-432.

Achard, P., Gong, F., Cheminant, S., Alioua, M., Hedden, P. and Genschik, P. (2008) The cold-inducible CBF1 factor-dependent signaling pathway modulates the accumulation of the growth-repressing DELLA proteins via its effect on gibberellin metabolism. *Plant Cell* **20**, 2117-2129.

Alpert, P. (2006). Constraints of tolerance: why are desiccation-tolerant organisms so small or rare? J Exp Biol **209,** 1575-1584.

Ando, E., Ohnishi, M., Wang, Y., Matsushita, T., Watanabe, A., Hayashi, Y., et al. (2013). TWIN SISTER OF FT, GIGANTEA, and CONSTANS have a positive but indirect effect on blue light-induced stomatal opening in Arabidopsis. Plant Physiol **162,** 1529-1538.

Baudry, A., Ito, S., Song, Y.H., Strait, A.A., Kiba, T., Lu, S., et al. (2010). F-box proteins FKF1 and LKP2 act in concert with ZEITLUPE to control Arabidopsis clock progression. Plant Cell **22,** 606-622.

Bechtold, N., Ellis, J., and Pelletier, G. (1993). In planta Agrobacterium mediated gene transfer by infiltration of adult Arabidopsis thaliana plants. C. R. Acad. Sci. Paris, Life Sci. **316,** 1194-1199.

Chinnusamy, V., Ohta, M., Kanrar, S., Lee, B.H., Hong, X., Agarwal, M., et al. (2003). ICE1: a regulator of cold-induced transcriptome and freezing tolerance in Arabidopsis. Genes Dev **17,** 1043-1054.

Chow, B.Y., and Kay, S.A. (2013). Global approaches for telling time: omics and the Arabidopsis circadian clock. Semin Cell Dev Biol **24,** 383-392.

Condon, A.G., Richards, R.A., and Farguhar, G.D. (1987). Carbon isotope discrimination is positively correlated with grain yield and dry matter production in field-grown wheat. Crop Sci. **27,** 996-1001.

Dodd, A.N., Salathia, N., Hall, A., Kevei, E., Toth, R., Nagy, F., et al. (2005). Plant circadian clocks increase photosynthesis, growth, survival, and competitive advantage. Science **309,** 630-633.

Endo, M., Shimizu, H., Nohales, M.A., Araki, T., and Kay, S.A. (2014). Tissue-specific clocks in Arabidopsis show asymmetric coupling. Nature **515,** 419-422.

Fargione, J., Hill, J., Tilman, D., Polasky, S., and Hawthorne, P. (2008). Land clearing and the biofuel carbon debt. Science **319,** 1235-1238.

Fornara, F., Panigrahi, K.C., Gissot, L., Sauerbrunn, N., Ruhl, M., Jarillo, J.A., et al. (2009). Arabidopsis DOF transcription factors act redundantly to reduce CONSTANS expression and are essential for a photoperiodic flowering response. Dev Cell **17,** 75-86.

Fornara, F., de Montaigu, A., Sanchez-Villarreal, A., Takahashi, Y., van Themaat, E.V., Huettel, B., et al. (2015). The GI-CDF module of Arabidopsis affects freezing tolerance and growth as well as flowering. Plant J.

Fowler, S.G., Cook, D., and Thomashow, M.F. (2005). Low temperature induction of Arabidopsis CBF1, 2, and 3 is gated by the circadian clock. Plant Physiol **137,** 961-968.

Fukushima, A., Kusano, M., Nakamichi, N., Kobayashi, M., Hayashi, N., Sakakibara, H., et al. (2009). Impact of clock-associated Arabidopsis pseudo-response regulators in metabolic coordination. Proc Natl Acad Sci U S A **106,** 7251-7256.

Garner, W.W., and Allard, H.A. (1920). Effect of the relative length of day and night and other factors of the environment on growth and reproduction in plants. J. Agr. Res. **18,** 553-606.

Gendron, J.M., Pruneda-Paz, J.L., Doherty, C.J., Gross, A.M., Kang, S.E., and Kay, S.A. (2012). Arabidopsis circadian clock protein, TOC1, is a DNA-binding transcription factor. Proc Natl Acad Sci U S A **109,** 3167-3172.

Harmer, S.L., Hogenesch, J.B., Straume, M., Chang, H.S., Han, B., Zhu, T., et al. (2000). Orchestrated transcription of key pathways in Arabidopsis by the circadian clock. Science **290,** 2110-2113.

Hicks, K.A., Millar, A.J., Carre, I.A., Somers, D.E., Straume, M., Meeks-Wagner, D.R., et al. (1996). Conditional circadian dysfunction of the Arabidopsis early-flowering 3 mutant. Science **274,** 790-792.

Huang, W., Perez-Garcia, P., Pokhilko, A., Millar, A.J., Antoshechkin, I., Riechmann, J.L., et al. (2012). Mapping the core of the Arabidopsis circadian clock defines the network structure of the oscillator. Science **336,** 75-79.

Imaizumi, T., Tran, H.G., Swartz, T.E., Briggs, W.R., and Kay, S.A. (2003). FKF1 is essential for photoperiodic-specific light signalling in Arabidopsis. Nature **426,** 302-306.

Imaizumi, T., Schultz, T.F., Harmon, F.G., Ho, L.A., and Kay, S.A. (2005). FKF1 F-box protein mediates cyclic degradation of a repressor of CONSTANS in Arabidopsis. Science **309,** 293-297.

Jaglo-Ottosen, K.R., Gilmour, S.J., Zarka, D.G., Schabenberger, O., and Thomashow, M.F. (1998). Arabidopsis CBF1 overexpression induces COR genes and enhances freezing tolerance. Science **280,** 104-106.

Kasuga, M., Liu, Q., Miura, S., Yamaguchi-Shinozaki, K., and Shinozaki, K. (1999). Improving plant drought, salt, and freezing tolerance by gene transfer of a single stress-inducible transcription factor. Nat Biotechnol **17,** 287-291.

Kebeish, R., Niessen, M., Thiruveedhi, K., Bari, R., Hirsch, H.J., Rosenkranz, R., et al. (2007). Chloroplastic photorespiratory bypass increases photosynthesis and biomass production in Arabidopsis thaliana. Nat Biotechnol **25,** 593-599.

Kim, W.Y., Fujiwara, S., Suh, S.S., Kim, J., Kim, Y., Han, L., et al. (2007). ZEITLUPE is a circadian photoreceptor stabilized by GIGANTEA in blue light. Nature **449,** 356-360.

Kim, W.Y., Ali, Z., Park, H.J., Park, S.J., Cha, J.Y., Perez-Hormaeche, J., et al. (2013). Release of SOS2 kinase from sequestration with GIGANTEA determines salt tolerance in Arabidopsis. Nat Commun **4,** 1352.

Kimura, Y., Aoki, S., Ando, E., Kitatsuji, A., Watanabe, A., Ohnishi, M., et al. (2015). A Flowering Integrator, SOC1, Affects Stomatal Opening in Arabidopsis thaliana. Plant Cell Physiol.

Kinoshita, T., Ono, N., Hayashi, Y., Morimoto, S., Nakamura, S., Soda, et al. (2011). FLOWERING LOCUS T regulates stomatal opening. Curr Biol **21,** 1232-1238.

Kobayashi, Y., Kaya, H., Goto, K., Iwabuchi, M., and Araki, T. (1999). A pair of related genes with antagonistic roles in mediating flowering signals. Science **286,** 1960-1962.

Kojima, S., Banno, H., Yoshioka, Y., Oka, A., Machida, C., and Machida, Y. (1999). A binary vector plasmid for gene expression in plant cells that is stably maintained in Agrobacterium cells. DNA Res **6,** 407-410.

Kojima, S., Takahashi, Y., Kobayashi, Y., Monna, L., Sasaki, T., Araki, T., et al. (2002). Hd3a, a rice ortholog of the Arabidopsis FT gene, promotes transition to flowering downstream of Hd1 under short-day conditions. Plant Cell Physiol **43,** 1096-1105.

Koo, B.H., Yoo, S.C., Park, J.W., Kwon, C.T., Lee, B.D., An, G., Zhang, Z., et al. (2013). Natural variation in OsPRR37 regulates heading date and contributes to rice cultivation at a wide range of latitudes. Mol Plant **6,** 1877-1888.

Langmead, B., Trapnell, C., Pop, M., and Salzberg, S.L. (2009). Ultrafast and memory-efficient alignment of short DNA sequences to the human genome. Genome Biol **10,** R25.

Leister, D., Varotto, C., Pesaresi, P., Niwergall, A., and Salamini, F. (1999). Large-scale evaluation of plant growth in Arabidopsis thaliana by non-invasive image analysis. Plant Physiol. Biochem **37,** 671-678.

Li, H., Handsaker, B., Wysoker, A., Fennell, T., Ruan, J., Homer, N., et al. (2009). The Sequence Alignment/Map format and SAMtools. Bioinformatics **25,** 2078-2079.

Liu, Q., Kasuga, M., Sakuma, Y., Abe, H., Miura, S., Yamaguchi-Shinozaki, K., et al. (1998). Two transcription factors, DREB1 and DREB2, with an EREBP/AP2 DNA binding domain separate two cellular signal transduction pathways in drought- and low-temperature-responsive gene expression, respectively, in Arabidopsis. Plant Cell **10,** 1391-1406.

Liu, T., Carlsson, J., Takeuchi, T., Newton, L., and Farre, E.M. (2013). Direct regulation of abiotic responses by the Arabidopsis circadian clock component PRR7. Plant J **76,** 101-114.

Maruyama, K., Sakuma, Y., Kasuga, M., Ito, Y., Seki, M., Goda, H., et al. (2004). Identification of cold-inducible downstream genes of the Arabidopsis DREB1A/CBF3 transcriptional factor using two microarray systems. Plant J **38,** 982-993.

Mir, R.R., Zaman-Allah, M., Sreenivasulu, N., Trethowan, R., and Varshney, R.K. (2012). Integrated genomics, physiology and breeding approaches for improving drought tolerance in crops. Theor Appl Genet **125,** 625-645.

Miyazaki, Y., Abe, H., Takase, T., Kobayashi, M., and Kiyosue, T. (2015). Overexpression of LOV KELCH PROTEIN 2 confers dehydration tolerance and is associated with enhanced expression of dehydration-inducible genes in Arabidopsis thaliana. Plant Cell Rep **34**, 843-852.

Murashige, T., and Skoog, F. (1962). A revised medium for rapid growth and bio-assays with tobacco tissue culture. Physiol Plant **15,** 473-497.

Murphy, R.L., Klein, R.R., Morishige, D.T., Brady, J.A., Rooney, W.L., Miller, F.R., et al. (2011). Coincident light and clock regulation of pseudoresponse regulator protein 37 (PRR37) controls photoperiodic flowering in sorghum. Proc Natl Acad Sci U S A **108,** 16469-16474.

Nakamichi, N., Kita, M., Ito, S., Yamashino, T., and Mizuno, T. (2005). PSEUDO-RESPONSE REGULATORS, PRR9, PRR7 and PRR5, together play essential roles close to the circadian clock of Arabidopsis thaliana. Plant Cell Physiol **46,** 686-698.

Nakamichi, N., Kita, M., Niinuma, K., Ito, S., Yamashino, T., Mizoguchi, T., et al. (2007). Arabidopsis clock-associated pseudo-response regulators PRR9, PRR7 and PRR5 coordinately and positively regulate flowering time through the canonical CONSTANS-dependent photoperiodic pathway. Plant Cell Physiol **48,** 822-832.

Nakamichi, N., Kusano, M., Fukushima, A., Kita, M., Ito, S., Yamashino, T., et al. (2009). Transcript profiling of an Arabidopsis PSEUDO RESPONSE REGULATOR arrhythmic triple mutant reveals a role for the circadian clock in cold stress response. Plant Cell Physiol **50,** 447-462.

Nakamichi, N., Kiba, T., Henriques, R., Mizuno, T., Chua, N.H., and Sakakibara, H. (2010). PSEUDO-RESPONSE REGULATORS 9, 7, and 5 are transcriptional repressors in the Arabidopsis circadian clock. Plant Cell **22,** 594-605.

Nakamichi, N. (2011). Molecular mechanisms underlying the Arabidopsis circadian clock. Plant Cell Physiol **52,** 1709-1718.

Nakamichi, N., Kiba, T., Kamioka, M., Suzuki, T., Yamashino, T., Higashiyama, T., et al. (2012). Transcriptional repressor PRR5 directly regulates clock-output pathways. Proc Natl Acad Sci U S A **109,** 17123-17128.

Ni, Z., Kim, E.D., Ha, M., Lackey, E., Liu, J., Zhang, Y., et al. (2009). Altered circadian rhythms regulate growth vigour in hybrids and allopolyploids. Nature **457,** 327-331.

Niinuma, K., Nakamich, N., Miyata, K., Mizuno, T., Kamada, H., and Mizuguchi, T. (2008). Roles of Arabidopsis PSEUDO-RESPONSE REGULATOR (PRR) genes in the opposite controls of flowering time and organ elongation under long-day and continuous light conditions. Plant Biotechnology **25,** 165–172.

Pin, P.A., Zhang, W., Vogt, S.H., Dally, N., Buttner, B., Schulze-Buxloh, G., et al. (2012). The role of a pseudo-response regulator gene in life cycle adaptation and domestication of beet. Curr Biol **22,** 1095-1101.

Redei, G. (1962). Supervital mutants of Arabidopsis Genetics **47,** 443-460.

Sato, E., Nakamichi, N., Yamashino, T., and Mizuno, T. (2002). Aberrant expression of the Arabidopsis circadian-regulated APRR5 gene belonging to the APRR1/TOC1 quintet results in early flowering and hypersensitiveness to light in early photomorphogenesis. Plant Cell Physiol **43,** 1374-1385.

Sawa, M., Nusinow, D.A., Kay, S.A., and Imaizumi, T. (2007). FKF1 and GIGANTEA complex formation is required for day-length measurement in Arabidopsis. Science **318,** 261-265.

Schmalenbach, I., Zhang, L., Reymond, M., and Jimenez-Gomez, J.M. (2014). The relationship between flowering time and growth responses to drought in the Arabidopsis Landsberg erecta x Antwerp-1 population. Front Plant Sci **5,** 609.

Song, Y.H., Smith, R.W., To, B.J., Millar, A.J., and Imaizumi, T. (2012). FKF1 conveys timing information for CONSTANS stabilization in photoperiodic flowering. Science **336,** 1045-1049.

Taji, T., Ohsumi, C., Iuchi, S., Seki, M., Kasuga, M., Kobayashi, M., et al. (2002). Important roles of drought- and cold-inducible genes for galactinol synthase in stress tolerance in Arabidopsis thaliana. Plant J **29,** 417-426.

Takata, N., Saito, S., Saito, C.T., and Uemura, M. (2010). Phylogenetic footprint of the plant clock system in angiosperms: evolutionary processes of pseudo-response regulators. BMC Evol Biol **10,** 126.

Tseng, T.S., Salome, P.A., McClung, C.R., and Olszewski, N.E. (2004). SPINDLY and GIGANTEA interact and act in Arabidopsis thaliana pathways involved in light responses, flowering, and rhythms in cotyledon movements. Plant Cell **16,** 1550-1563.

Tsukagoshi, H., Busch, W., and Benfey, P.N. (2010). Transcriptional regulation of ROS controls transition from proliferation to differentiation in the root. Cell **143,** 606-616.

Turner, A., Beales, J., Faure, S., Dunford, R.P., and Laurie, D.A. (2005). The pseudo-response regulator Ppd-H1 provides adaptation to photoperiod in barley. Science **310,** 1031-1034.

Valverde, F., Mouradov, A., Soppe, W., Ravenscroft, D., Samach, A., and Coupland, G. (2004). Photoreceptor regulation of CONSTANS protein in photoperiodic flowering. Science **303,** 1003-1006.

Wang, L., Kim, J., and Somers, D.E. (2013). Transcriptional corepressor TOPLESS complexes with pseudoresponse regulator proteins and histone deacetylases to regulate circadian transcription. Proc Natl Acad Sci U S A **110,** 761-766.

Wang, Y., Noguchi, K., Ono, N., Inoue, S., Terashima, I., and Kinoshita, T. (2014). Overexpression of plasma membrane H+-ATPase in guard cells promotes light-induced stomatal opening and enhances plant growth. Proc Natl Acad Sci U S A **111,** 533-538.

Xue, W., Xing, Y., Weng, X., Zhao, Y., Tang, W., Wang, L., et al. (2008). Natural variation in Ghd7 is an important regulator of heading date and yield potential in rice. Nat Genet **40,** 761-767.

Yamaguchi-Shinozaki, K., and Shinozaki, K. (2006). Transcriptional regulatory networks in cellular responses and tolerance to dehydration and cold stresses. Annu Rev Plant Biol **57,** 781-803.

Yan, W., Liu, H., Zhou, X., Li, Q., Zhang, J., Lu, L., et al. (2013). Natural variation in Ghd7.1 plays an important role in grain yield and adaptation in rice. Cell Res **23,** 969-971.

Yanovsky, M.J., and Kay, S.A. (2002). Molecular basis of seasonal time measurement in Arabidopsis. Nature **419,** 308-312.
Yuan, Q., Saito, H., Okumoto, Y., Inoue, H., Nishida, H., Tsukiyama, T., et al. (2009). Identification of a novel gene ef7 conferring an extremely long basic vegetative growth phase in rice. Theor Appl Genet **119,** 675-684.

Legends to Figures

Figure 1. Biomass of PRR5-VP-expressing Arabidopsis (PRR5-VP). (A) Total dry weight of Arabidopsis grown under LD. (B) Flowering time of Arabidopsis grown under LD. (C) Leaf surface area plotted against days after germination (DAG) until flowering. (D) Representatives of (C). White bars indicate 1 cm. (E) CO_2 assimilation rate and (F) stomatal conductance of plants just before flowering. Error bars indicate SE of 8 to 15 biological replicates (for A to C), and 3 biological replicates (E and F). Asterisks indicate significant difference from wild-type (Student's t test $p < 0.05$).

Figure 2. Flowering time of PRR7-VP and TOC1-VP. (A) Flowering time of plants grown under long-day conditions. Scale bar indicates 5 cm. Error bars indicate SD of 12 plants. Asterisks indicate significant difference from wild-type (Student's t test $p < 0.05$). Expression of (B) *FT*, (C) *CO*, (D) *GI*, (E) *FKF1*, (F) *CDF1*, (G) *CDF2*, (H) *CDF3*, and (I) *CDF5* in plants grown under LD conditions. Error bars indicate SD of three technical replicates. Grey areas indicate dark periods. Similar results for (A) to (I) were obtained from an independent experiment.

Figure 3. Genome-wide gene expression analysis of PRR5-VP. eGO analysis for up-regulated genes (A) or down-regulated genes (B) in PRR5-VP compared to wild-type. Plants were grown under 12 h light / 12 h dark cycles.

Figure 4. Cold, salt, and drought stress tests. Wild-type, *prr9 prr7 prr5*, PRR5-VP, and *PRR5-ox* Arabidopsis were incubated at -5˚C for 1 day (A), drought stress for 16 days (B), or 200 mM NaCl for 6 days (C). Wild-type, *prr9 prr7 prr5*, *PRR5-VP*, *ft tsf*, and *gi* were subjected to drought stresses for 17 days (D), or 200 mM NaCl for 4 days (E). Error bars indicate SE of three independent experiments. Asterisks show significant differences from wild-type (Student's t test $p < 0.05$). White bars in (A), (C), and (E) are 1 cm, and in (B) and (D) are 5 cm.

Figure 5. Expression of *DREB1* genes and DREB1-downstream genes in PRR5-VP. (A) *DREB1* genes expression under 12 h light / 12 h dark cycle and constant light (LL) conditions. Black and gray lines indicate gene expression in wild-type and PRR5-VP, respectively. Gray area indicates dark period. (B) Expression of *DREB1* genes and DREB1-downstream genes in plants grown under 12 h light / 12 h dark conditions. Time indicates hours after 'lights on'. Black asterisks indicate up-regulated genes in PRR5-VP compared with wild-type at a minimum of one time point (FDR $q < 0.01$). Red asterisks indicate *DREB1* genes. (C) Expression of *DREB1* genes in *ft tsf* and *gi* plants. Maximal expression in wild-type is set as 1.0, and gray area indicates dark period for (A) and (C). Error bars indicate SD of three biological (A) or technical replicates (C). Experiment of (C) was done twice using other biological replicates with similar results.

Figure 6. Possible molecular mechanism for the improvement in biomass and cold-, drought-, and salinity-stress responses of Arabidopsis plants containing PRR-VP. Black arrows and the negative bar (between *CDFs* and *CO*, *FT*) indicate direct transcriptional activation and repression, respectively.

Supplemental Figure 1. PRR7-VP and TOC-VP protein expression in transgenic Arabidopsis. Arrows indicate PRR7-VP and TOC1-VP in upper and lower panels, respectively. Asterisks indicate non-specific bands.

Supplemental Figure 2. Drought stress tests using plants of similar size. Water was withheld from PRR5-VP and wild-type plants for 14 d (A) or 16 d (B). Plant size before drought stress, and survival rates are shown in upper and lower panels. Error bars are SD.

Supplemental Figure 3. PRR5, PRR7, and TOC1 association profiles around *CDF1* (A) and *LHY* (B) regions in the Arabidopsis genome. ChIPseq data of PRR5-GFP (Nakamichi et al., 2012), PRR7-HA (Liu et al., 2013), and TOC1-YFP (Huang et al., 2012) were analyzed in the same analytical platform. Horizontal bars indicate 500 bp and 1,000 bp in (A) and (B), respectively. Numbers behind vertical scale bars indicate sequence reads. Colored positions indicate a nucleotide mismatch to the reference genomic sequence.

Supplemental Figure 4. Expression of *ICE1*. *ICE1* expression in PRR5-VP was determined by ATH1 microarray. *ICE1* expression in PRR5-VP and wild-type was not significantly different (FDR $q > 0.1$). Error bars indicate SD of three biological replicates.

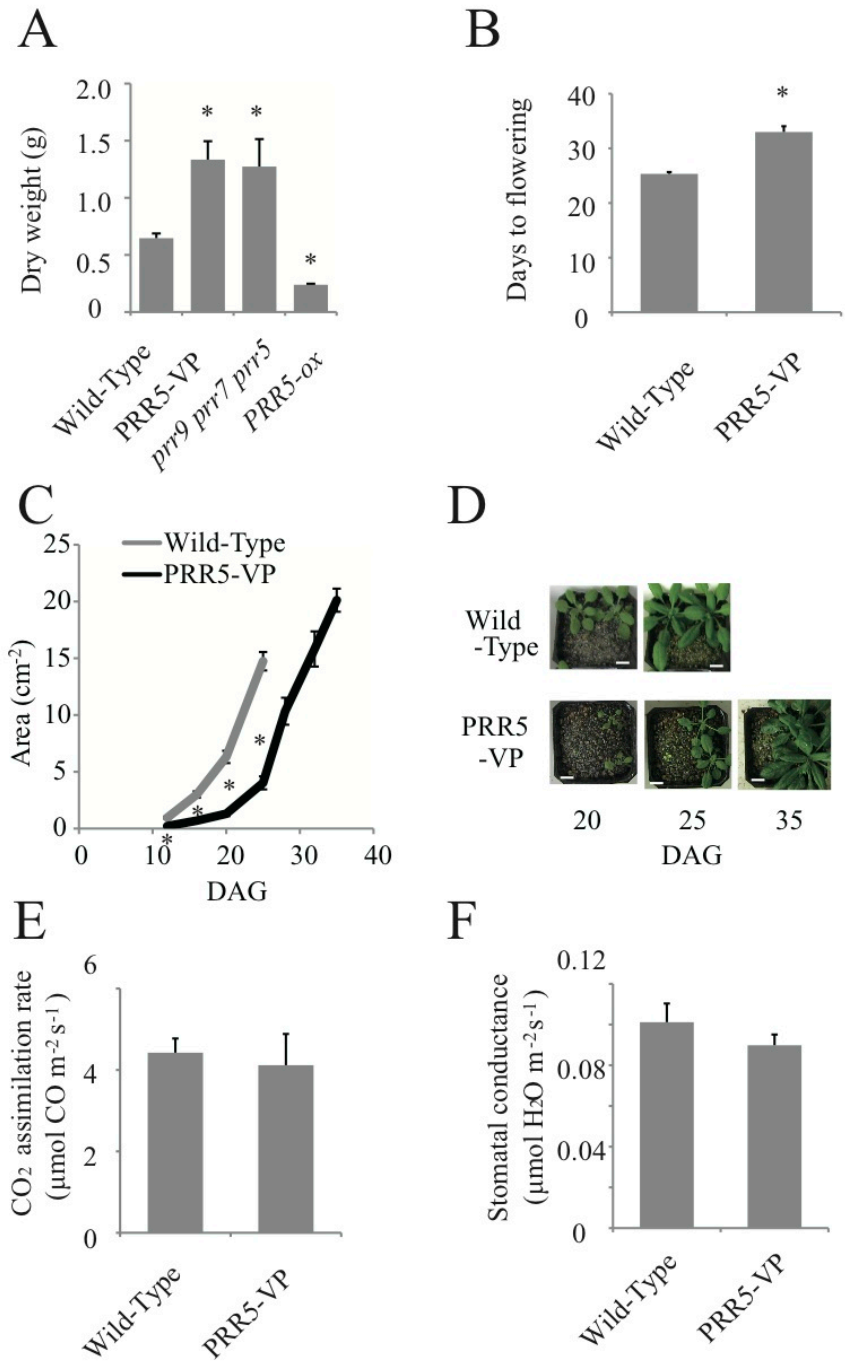
A
Dry weight (g)
2.0
1.5
1.0
0.5
0
Wild-Type
PRR5-VP
prr9 prr7 prr5
PRR5-ox
B
Days to flowering
40
30
20
10
0
Wild-Type
PRR5-VP
C
Wild-Type
PRR5-VP
Area (cm-2)
25
20
15
10
5
0
0
10
20
30
40
DAG
D
Wild -Type
PRR5 -VP
20
25
35
DAG
E
CO2 assimilation rate (µmol CO m-2 s-1)
6
4
2
0
Wild-Type
PRR5-VP
F
Stomatal conductance (µmol H2O m-2 s-1)
0.12
0.08
0.04
0
Wild-Type
PRR5-VP

Figure 1

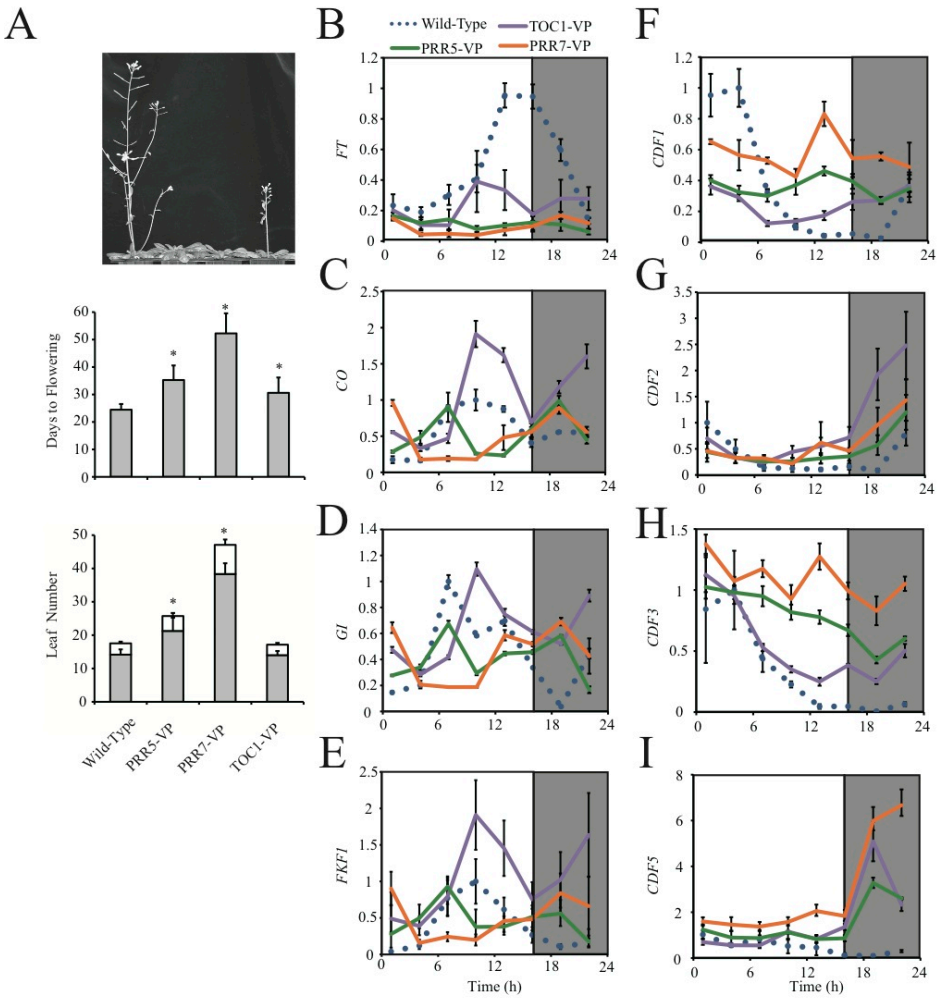
A
B
C
D
E
F
G
H
I
Wild-Type
TOC1-VP
PRR5-VP
PRR7-VP
Days to Flowering
Leaf Number
Wild-Type
PRR5-VP
PRR7-VP
TOC1-VP
FT
CO
GI
FKF1
CDF1
CDF2
CDF3
CDF5
Time (h)
Time (h)

Figure 2

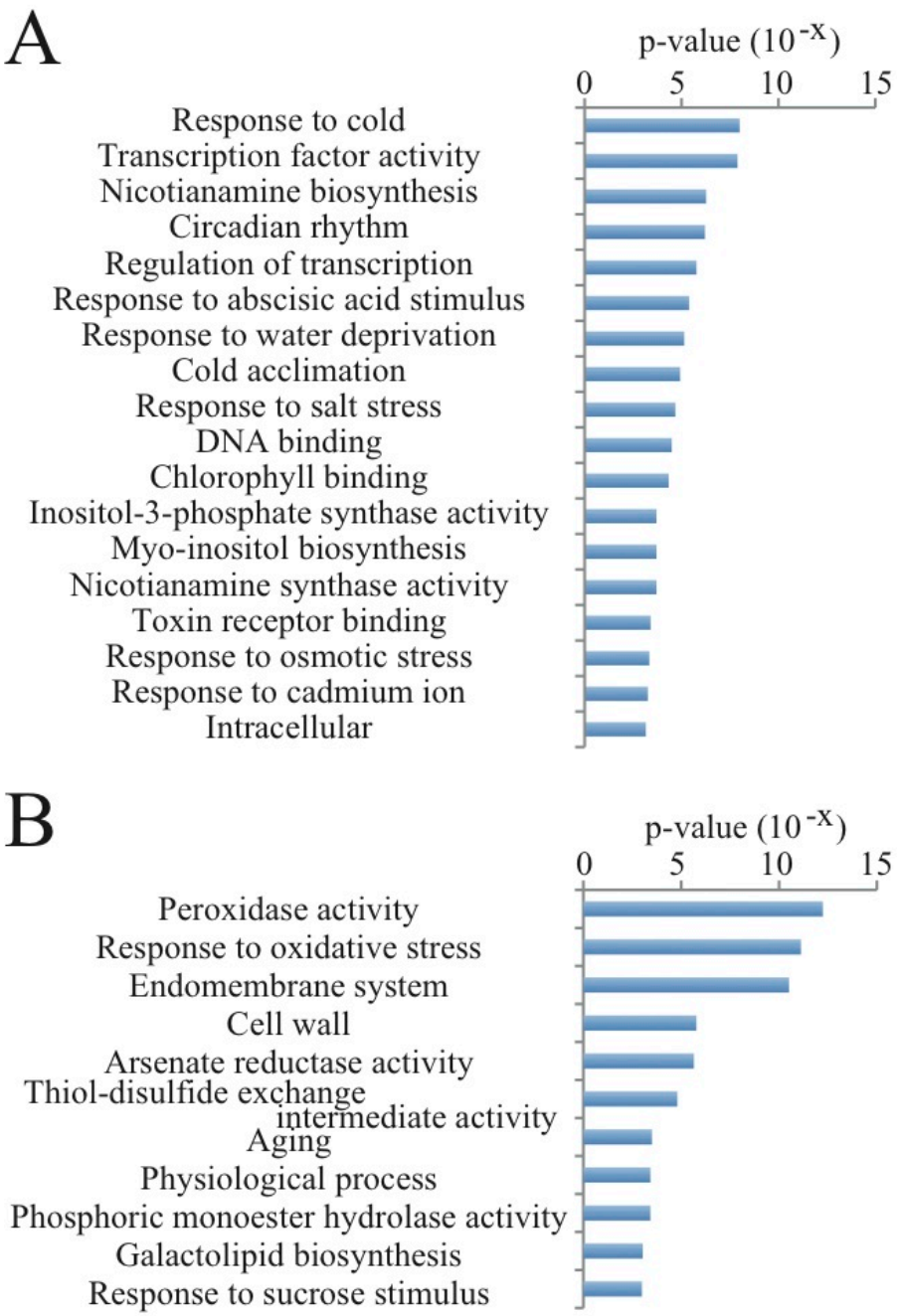
A
p-value (10^{-x})
0
5
10
15
Response to cold
Transcription factor activity
Nicotianamine biosynthesis
Circadian rhythm
Regulation of transcription
Response to abscisic acid stimulus
Response to water deprivation
Cold acclimation
Response to salt stress
DNA binding
Chlorophyll binding
Inositol-3-phosphate synthase activity
Myo-inositol biosynthesis
Nicotianamine synthase activity
Toxin receptor binding
Response to osmotic stress
Response to cadmium ion
Intracellular
B
p-value (10^{-x})
0
5
10
15
Peroxidase activity
Response to oxidative stress
Endomembrane system
Cell wall
Arsenate reductase activity
Thiol-disulfide exchange intermediate activity
Aging
Physiological process
Phosphoric monoester hydrolase activity
Galactolipid biosynthesis
Response to sucrose stimulus

Figure 3

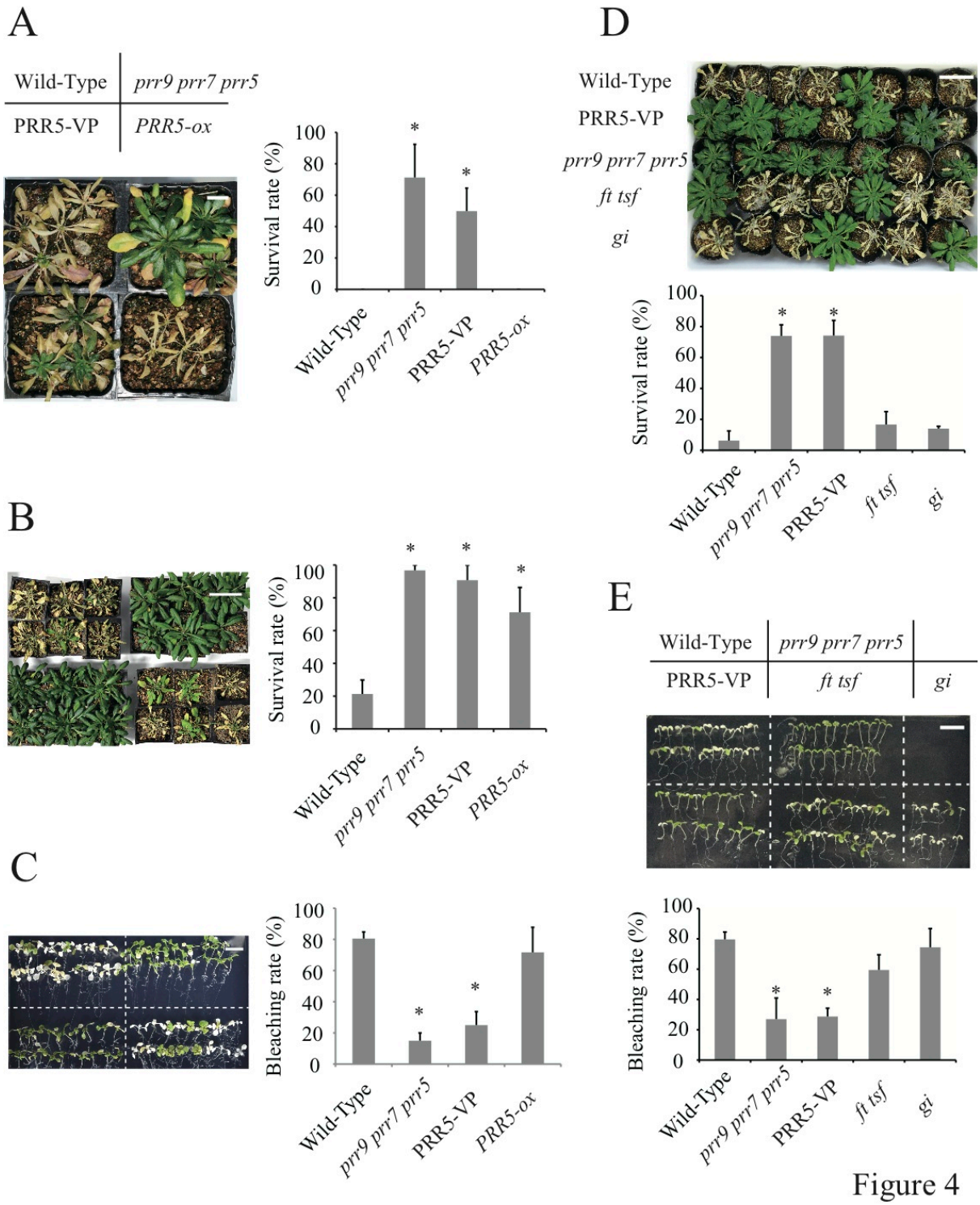
A
Wild-Type
prr9 prr7 prr5
PRR5-VP
PRR5-ox
Survival rate (%)
100
80
60
40
20
0
*
*
Wild-Type
prr9 prr7 prr5
PRR5-VP
PRR5-ox
B
Survival rate (%)
100
80
60
40
20
0
*
*
*
Wild-Type
prr9 prr7 prr5
PRR5-VP
PRR5-ox
C
Bleaching rate (%)
100
80
60
40
20
0
*
*
Wild-Type
prr9 prr7 prr5
PRR5-VP
PRR5-ox
D
Wild-Type
PRR5-VP
prr9 prr7 prr5
ft tsf
gi
Survival rate (%)
100
80
60
40
20
0
*
*
Wild-Type
prr9 prr7 prr5
PRR5-VP
ft tsf
gi
E
Wild-Type
prr9 prr7 prr5
PRR5-VP
ft tsf
gi
Bleaching rate (%)
100
80
60
40
20
0
*
*
Wild-Type
prr9 prr7 prr5
PRR5-VP
ft tsf
gi

Figure 4

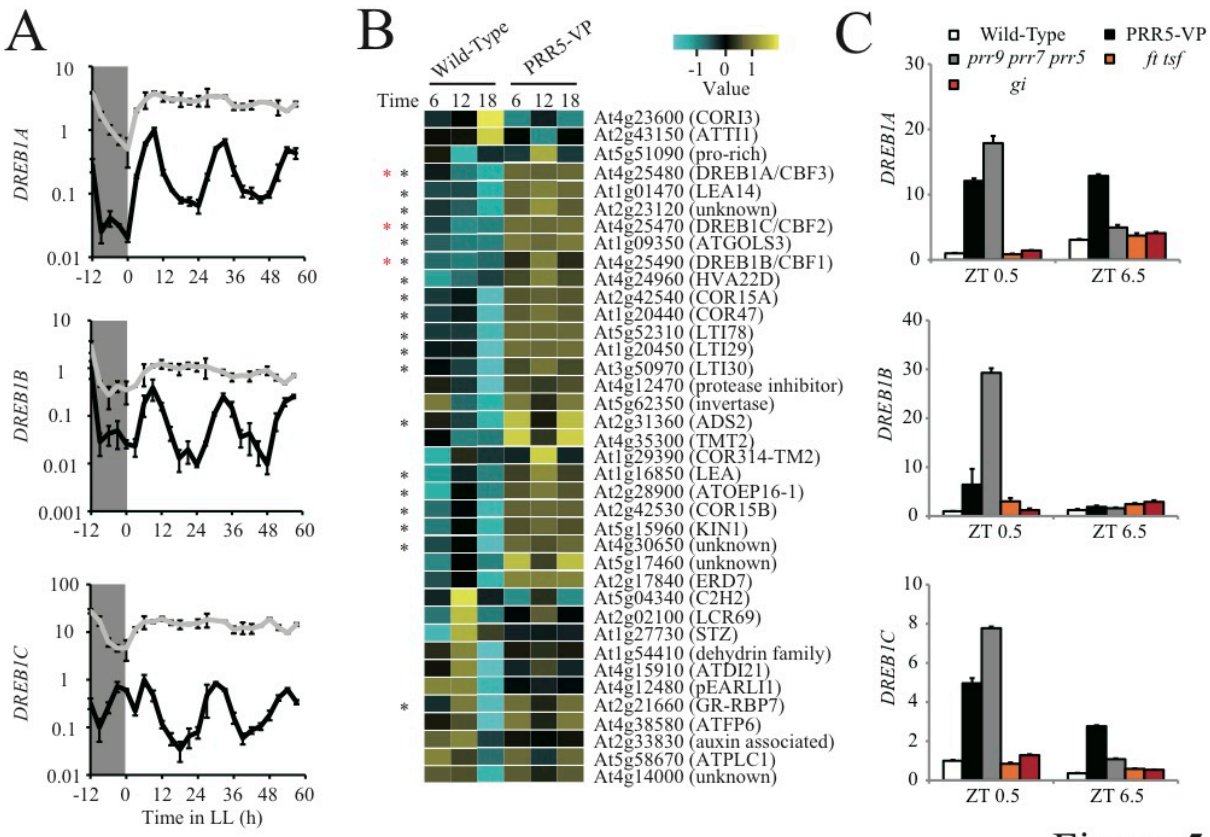
A
DREB1A
DREB1B
DREB1C
Time in LL (h)
B
Wild-Type
PRR5-VP
Time 6 12 18 6 12 18
Value
At4g23600 (CORI3)
At2g43150 (ATTI1)
At5g51090 (pro-rich)
At4g25480 (DREB1A/CBF3)
At1g01470 (LEA14)
At2g23120 (unknown)
At4g25470 (DREB1C/CBF2)
At1g09350 (ATGOLS3)
At4g25490 (DREB1B/CBF1)
At4g24960 (HVA22D)
At2g42540 (COR15A)
At1g20440 (COR47)
At5g52310 (LTI78)
At1g20450 (LTI29)
At3g50970 (LTI30)
At4g12470 (protease inhibitor)
At5g62350 (invertase)
At2g31360 (ADS2)
At4g35300 (TMT2)
At1g29390 (COR314-TM2)
At1g16850 (LEA)
At2g28900 (ATOEP16-1)
At2g42530 (COR15B)
At5g15960 (KIN1)
At4g30650 (unknown)
At5g17460 (unknown)
At2g17840 (ERD7)
At5g04340 (C2H2)
At2g02100 (LCR69)
At1g27730 (STZ)
At1g54410 (dehydrin family)
At4g15910 (ATDI21)
At4g12480 (pEARLI1)
At2g21660 (GR-RBP7)
At4g38580 (ATFP6)
At2g33830 (auxin associated)
At5g58670 (ATPLC1)
At4g14000 (unknown)
C
Wild-Type
PRR5-VP
prr9 prr7 prr5
ft tsf
gi
DREB1A
DREB1B
DREB1C
ZT 0.5
ZT 6.5

Figure 5

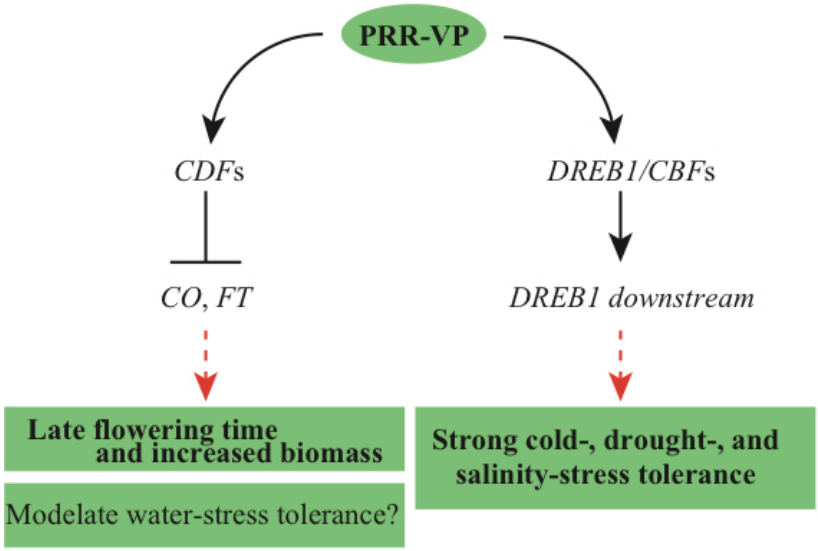
PRR-VP
CDFs
DREB1/CBFs
CO, FT
DREB1 downstream
Late flowering time and increased biomass
Modelate water-stress tolerance?
Strong cold-, drought-, and salinity-stress tolerance

Figure 6

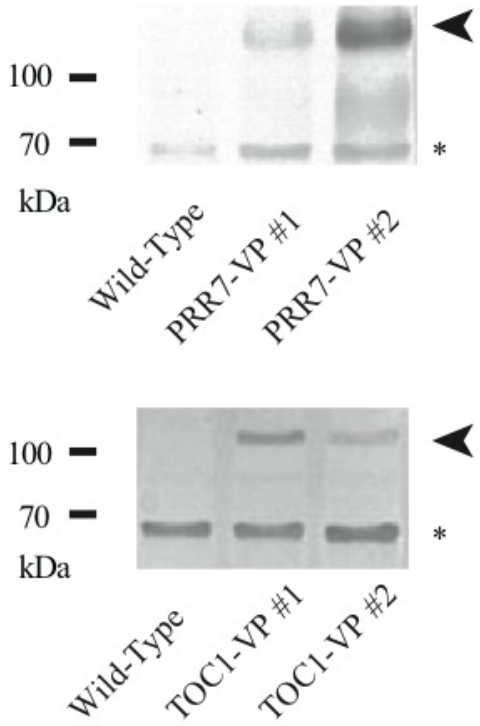

Supplemental Figure 1. PRR7-VP and TOC-VP protein expression in transgenic *Arabidopsis*. Arrows indicate PRR7-VP and TOC1-VP in upper and lower panels, respectively. Asterisks indicate non-specific bands.

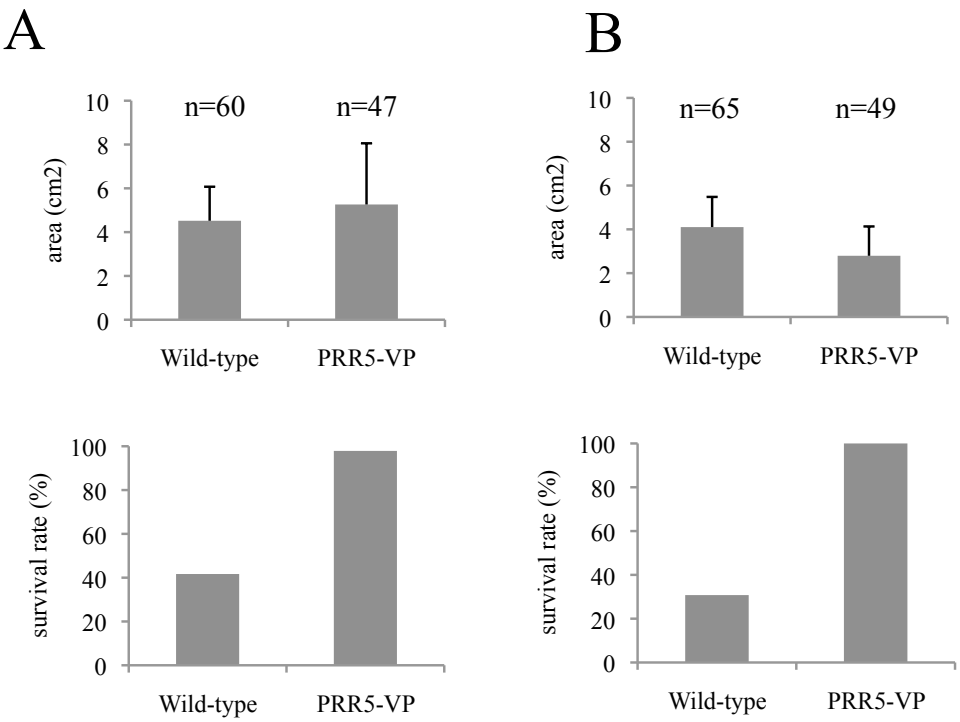

Supplemental Figure 2. Drought stress tests using the similar size of plants. PRR5-VP and wild-type were subjected to unwatering for 14 d (A) or 16 d (B). Plant size before drought stress, and survival rate were shown in upper and lower panels. Error bars are SD.

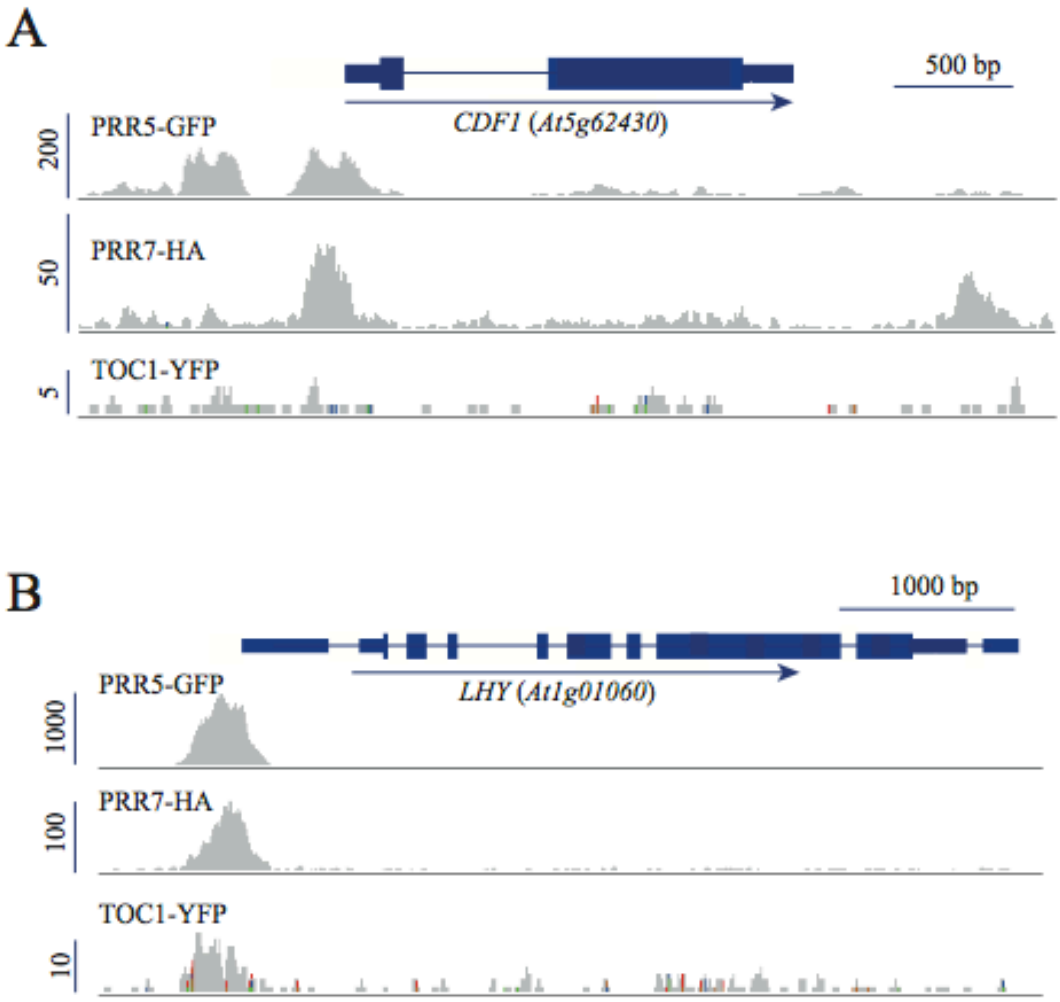

Supplemental Figure 3. PRR5, PRR7, and TOC1 association profiles around *CDF1* (A) and *LHY* (B) regions in the *Arabidopsis* genome. ChIPseq data of PRR5-GFP (Nakamichi et al. 2012), PRR7-HA (Liu et al. 2013), and TOC1-YFP (Huang et al. 2012) were analyzed in the same analytical platform. Horizontal bars indicate 500 bp and 1,000 bp in (A) and (B), respectively. Numbers behind vertical scale bars indicate sequence reads. Colored positions indicate a nucleotide mismatch to the reference genomic sequence.

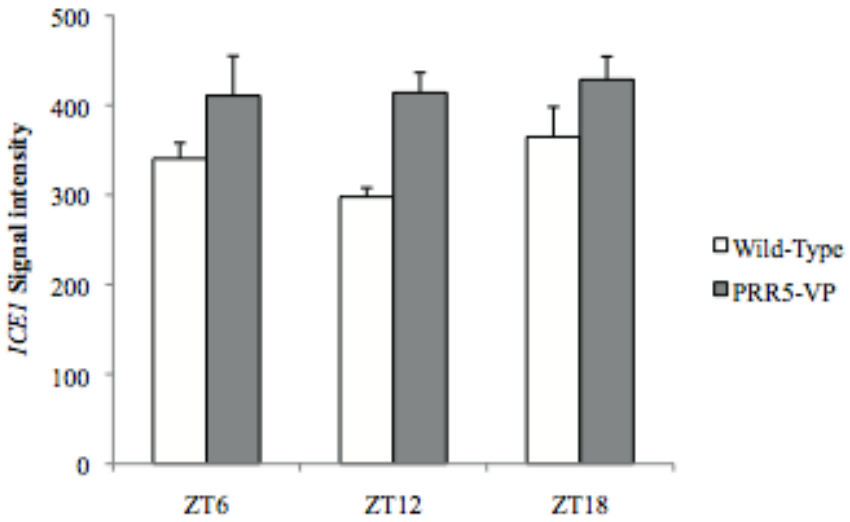

Supplemental Figure 4. Expression of *ICE1*. *ICE1* expression in PRR5-VP was determined by microarray. *ICE1* expression in PRR5-VP and wild-type was not significantly different (FDR q > 0.1). Error bars indicate SD of three biological replicates.